SCIENCE CHINA

Physics, Mechanics & Astronomy



Article

July 2023 Vol. 66 No. 7: 277511 https://doi.org/10.1007/s11433-022-2085-x

Light-induced magnetic phase transition in van der Waals antiferromagnets

Jiabin Chen^{1,2,3}, Yang Li³, Hongyu Yu^{1,2}, Yali Yang^{1,2}, Heng Jin³, Bing Huang^{3,4*}, and Hongjun Xiang^{1,2,5*}

² Shanghai Qi Zhi Institute, Shanghai 200030, China;

Received December 6, 2022; accepted February 22, 2023; published online May 6, 2023

Control over magnetic properties by optical stimulation is not only interesting from the physics point of view, but also important for practical applications such as magneto-optical devices. Here, based on a simple tight-binding (TB) model, we propose a general theory of light-induced magnetic phase transition (MPT) in antiferromagnets. Considering the fact that the bandgap of the antiferromagnetic (AFM) phase is usually larger than that of the ferromagnetic (FM) one for a given system, we suggest that light-induced electronic excitation prefers to stabilize the FM state over the AFM one, and will induce an MPT from AFM phase to FM phase once a critical photocarrier concentration (α_c) is reached. This theory has been confirmed by performing first-principles calculations on a series of 2D van der Waals (vdW) antiferromagnets. Interestingly, a linear relationship between α_c and the intrinsic material parameters is obtained, in agreement with our TB model analysis. Our general theory paves a new way to manipulate 2D magnetism with high speed and superior resolution.

first-principles calculation, density functional theory, two-dimensional materials, magnetic phase transition

PACS number(s): 71.15.Mb, 73.20.-r, 75.30.Kz

Citation: J. Chen, Y. Li, H. Yu, Y. Yang, H. Jin, B. Huang, and H. Xiang, Light-induced magnetic phase transition in van der Waals anti-ferromagnets, Sci. China-Phys. Mech. Astron. 66, 277511 (2023), https://doi.org/10.1007/s11433-022-2085-x

1 Introduction

Discovering long-range magnetism in two-dimensional (2D) materials is one of the most significant developments in the field of magnetism in recent years [1,2]. Once the magnetic phases in 2D magnets can be manipulated effectively, they can be widely applied to design nanoscale spintronic and

memory devices. Up to now, several methods were attempted to control 2D magnetism [3], including external electric [4], magnetic [5], and strain fields [6,7]. However, these methods are either applicable only for specific material systems or are not easy to control. Thus, developing easily accessible approaches for engineering magnetic phase transition (MPT) in 2D magnets remains highly desirable.

Illumination proved to be a remote, fast, and reversible way for tuning the physical properties of materials [8]. For example, it was found that superconductivity can be en-

¹ Key Laboratory of Computational Physical Sciences (Ministry of Education), Institute of Computational Physical Sciences, State Key Laboratory of Surface Physics, Department of Physics, Fudan University, Shanghai 200433, China;

³ Beijing Computational Science Research Center, Beijing 100193, China;

⁴ Department of Physics, Beijing Normal University, Beijing 100193, China;

⁵ Collaborative Innovation Center of Advanced Microstructures, Nanjing 210093, China

^{*}Corresponding authors (Bing Huang, email: bing.huang@csrc.ac.cn; Hongjun Xiang, email: hxiang@fudan.edu.cn)

hanced by illumination [9]. On subpicosecond timescales, the photoinduced insulator-metal transition can take place in vanadium dioxide [10]. For the magnetic properties, it was shown that light can attenuate the rhombohedral lattice distortion by rapidly weakening the magnetic order in NiO [11], and the light-induced ferromagnetism in non-magnetic moiré superlattices was observed [12]. Recently, all-optical switching of magnetization was found in three-layer CrI₃ which magnetization is flipped from an up to a down state [13]. In addition, light-induced demagnetization in ferromagnetic (FM) materials has also been observed experimentally [14] and investigated theoretically [15]. The ultrafast photoinduced low-spin (LS) and high-spin (HS) transition was discovered in several inorganic-organic compounds including the cyanide-bridged CoFe system [16]. Light-induced AFM-to-FM phase transition was observed in Pr_{0.6}La_{0.1}Ca_{0.3}MnO₃ thin films [17] but the microscopic mechanism remains unclear. Until now, light control of 2D magnetism is rather rare in experiments. In particular, a general theory for light-induced MPT is also lacking.

In this study, we first employ a simple tight-binding model to discover a general mechanism of the photoexcitation-induced AFM to FM phase transition. This mechanism is related to the fact that the bandgap of the AFM configuration is generally larger than that of the FM configuration. Using density functional theory (DFT) to obtain magnetic properties of the ground state and constrained density functional theory (cDFT, as described in ref. [18]) to mimic the thermalized photocarrier population, we propose that vdW layered antiferromagnets are the ideal platforms to study MPT under laser illumination. We demonstrate the phase transitions from AFM state to FM state in monolayer MnI₂

and MnP X_3 (X=S, Se, Te) and bilayer CrI₃, MnBi₂Te₄ when the photocarrier concentration n_e reaches the order of 10^{12} e⁻/cm², which is in the same order as the experimentally accessible photocarriers concentration (e.g., (2-3)×10¹² e⁻/cm² in 2D MoS₂ [19]).

2 Materials and method

We select the pseudo-potential Vienna *ab initio* simulation package (VASP) for the calculations of the electronic and magnetic properties [20]. The Perdew-Burke-Ernzerhof [21] version of the exchange-correlation potentials was utilized. The correlation effect caused by partially occupied 3*d* orbitals is corrected by GGA+*U* method [22]. The *U* values are set to be 3 eV in MnI₂, CuFeO₂, MnPX₃ (X=S, Se,Te), CrI₃ and MnBi₂Te₄. In DFT and GW-BSE calculations, the vacuum layer of the 4×4×1 MnI₂ supercell is set to 23 Å. Gamma-centered *k*-points grid is selected. The total number of energy bands is 400 and the number of valence and conduction bands used in BSE calculation are all 10.

2.1 General theory of light-induced MPT

As shown in Figure 1, to identify how the bandgap $(G_{\rm diff})$ difference and total energy difference $(E_{\rm diff})$ between AFM and FM configurations determine the ground state of the system, we introduce a two-site tight-binding model [23] to simulate the simplest magnetic semiconductor system. The mean-field Hamiltonians for the AFM and FM states are given as:

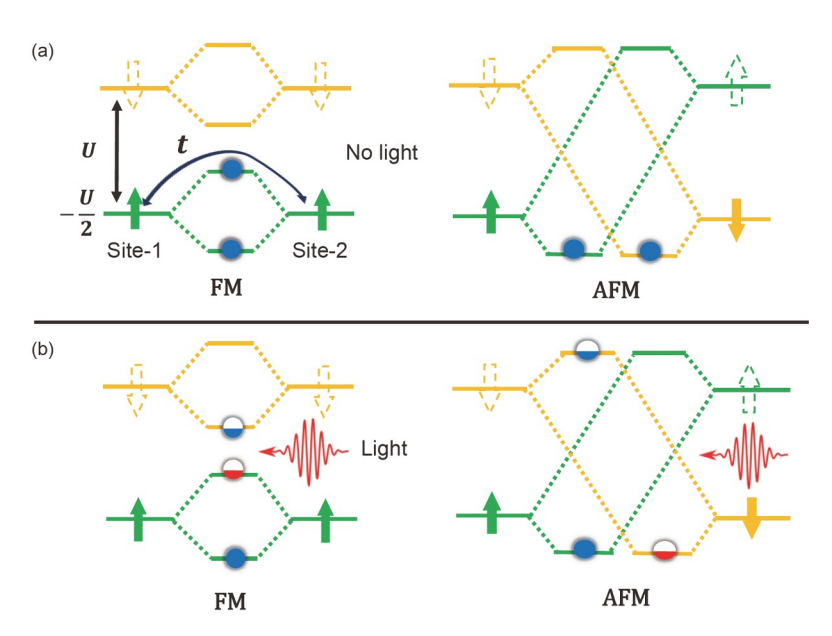


Figure 1 (Color online) Schematic diagrams of orbital evolution in a double-site model. (a) FM configuration with no light (left) and AFM configuration with no light (right). (b) FM configuration with light (left) and AFM configuration with light (right). Partial electrons were excited. Green and orange lines represent spin-up and spin-down orbitals, respectively. Blue and red dots represent electrons and holes, respectively.

$$H = -t \sum_{\sigma=\uparrow,\downarrow} \left(a_{1\sigma}^{+} a_{2\sigma} + h.c. \right) + \frac{U}{2} \sum_{i=1,2} e_{i} \left(a_{i\downarrow}^{+} a_{i\downarrow} - a_{i\uparrow}^{+} a_{i\uparrow} \right), (1)$$

where *i* represents the two neighboring magnetic sites, *U* represents the on-site repulsive energy and *t* represents the hopping integral which includes nonlinear properties like interlayer coupling in multilayer or bilayer materials, e_i (+1 or -1) denotes the spin direction of the *i*-th site. For the FM state, e_1 = e_2 =1, while e_1 =1 and e_2 =-1 for the AFM state. By diagonalizing the Hamiltonian and considering the usual condition of U>>t in semiconductors and insulators, we can get

$$E_{\rm AFM} = -\sqrt{U^2 + 4t^2} \approx -U - \frac{2t^2}{U}, E_{\rm FM} = -U,$$
 (2)

$$G_{AFM} = \sqrt{U^2 + 4t^2} \approx U + \frac{2t^2}{U}, G_{FM} = U - 2t,$$
 (3)

where $E_{\rm AFM}$ and $E_{\rm FM}$ represent the total energy in AFM and FM configurations respectively, $G_{\rm AFM}$ and $G_{\rm FM}$ represent the bandgap in AFM and FM configurations respectively. Consequently, we can obtain $E_{\rm diff}$ and $G_{\rm diff}$ between the AFM and FM states.

$$E_{\text{diff}} = E_{\text{AFM}} - E_{\text{FM}} = -\frac{2t^2}{U},\tag{4}$$

$$G_{\text{diff}} = G_{\text{AFM}} - G_{\text{FM}} = \frac{2t^2}{U} + 2t.$$
 (5)

As indicated in eq. (4), we can see that the energy of the AFM state is lower than that of the FM state, which is consistent with the fact that the kinetic exchange usually leads to an antiferromagnetic state. Interestingly, eq. (5) indicates that the bandgap of the FM state is smaller than that of the AFM state, in agreement with the fact that the FM state is usually more metallic (e.g., in colossal magnetoresistance (CMR) manganese oxides) [24,25].

We now assume that α number of electrons is photoexcited from the valence bands (VB) to the conduction bands (CB) under light illumination, then the new energy difference ($E'_{\rm diff}$) between the AFM and FM states becomes

$$E'_{\text{diff}} = E_{\text{diff}} + \alpha G_{\text{diff}} = -\frac{2t^2}{U} + \alpha \left(\frac{2t^2}{U} + 2t\right). \tag{6}$$

The critical condition is $E_{\rm diff}'=0$, i.e., $\alpha_c=-\frac{E_{\rm diff}}{G_{\rm diff}}$, which indicates that once $\alpha \geqslant \alpha_c$ electron is excited, and the magnetic phase transition from the AFM state to the FM state can be realized. Here we assume that the band structure change induced by photoexcitation is negligible which is reasonable as long as the photocarrier concentration is not large ($n_e << 1~{\rm e^-/f.u.}$). It is worth noting that the thermodynamic process rather than the dynamic process is considered here, i.e., the time-dependent electron spin transfer and flipping process are not included. This is because the system can always reach its lowest-energy magnetic state after a suffi-

ciently long relaxation time. Under illumination, the electrons will be excited from VB to CB in the order of 1 ns even in indirect bandgap semiconductors, and the excited high-energy electrons and holes will fall back to CB minimum (CBM) and VB maximum (VBM) in a shorter time (~1 ps), respectively. Furthermore, the timescale required for the photocarrier recombination (1 ns-1 µs) is much longer than that of excitation [26]. Given this fact, here we focus on the steady state with constant hole and electron concentration at VBM and CBM under persistent light illumination, without investigating the ultrafast response on the picosecond time scale. In addition, we consider the effect of paramagnetic states in the SM.

2.2 Light-induced MPT in monolayer MnI₂

Monolayer MnI₂ with the P-3m1 symmetry was reported to exhibit a screw-type AFM ground state. This magnetic structure induces ferroelectric polarization along the [110] direction of MnI₂ [27-29], which was explained by the general theory proposed for describing the ferroelectric polarization induced by a spin-spiral order [30]. Here, we propose that illumination can be adopted to realize the MPT in monolayer MnI₂. As shown in Figure 2(a), a simple stripetype collinear configuration is adopted for the AFM state in a $4 \times 4 \times 1$ supercell. As shown in Figure 2(b), the CBM and VBM of both AFM and FM states are mainly contributed by the cation Mn d and anion I p orbitals, respectively. Therefore, the photoexcited electron is transferred between the anion and cation. This is slightly different from the scenario described by the TB model (eq. (1)) where only cation orbitals are considered. However, it does not influence our main conclusion on MPT because it is based on the fact that the bandgap of AFM configuration is larger than that of FM configuration. Our DFT calculations show that E_{diff} and G_{diff} are -0.077 and 0.321 eV based on Figure 1(a) configurations, respectively. According to the model, we proposed (eq. (6)), the critical photocarrier for MPT is α_c =0.239 e⁻/f.u., which is equivalent to $5.015 \times 10^{12} \text{ e}^{-1}/\text{cm}^2$. When $\alpha \ge \alpha_c$, the total energy of the FM state will be lower than that of the AFM state. We confirm this result by performing the cDFT calculations where the presence of electrons and holes is explicitly taken into account. Our cDFT calculations indeed show that the total energy difference $E'_{\rm diff}$ is zero when we set $\alpha_c = 0.239 \text{ e}^{-}/\text{f.u.}$ for both FM state and AFM state (see the star point in Figure 2(c)). Besides, we verified that the lightinduced MPT between the non-collinear AFM state and FM state will also occur by considering a helical spin-spiral AFM state with q = (1/3, 0, 0) and q = (1/3, 1/3, 0) [25] (see Supporting Information). Noteworthy, we use the Ising model as an example to derive this phase transition theory, but it still applies when generalized to the spin spiral states,

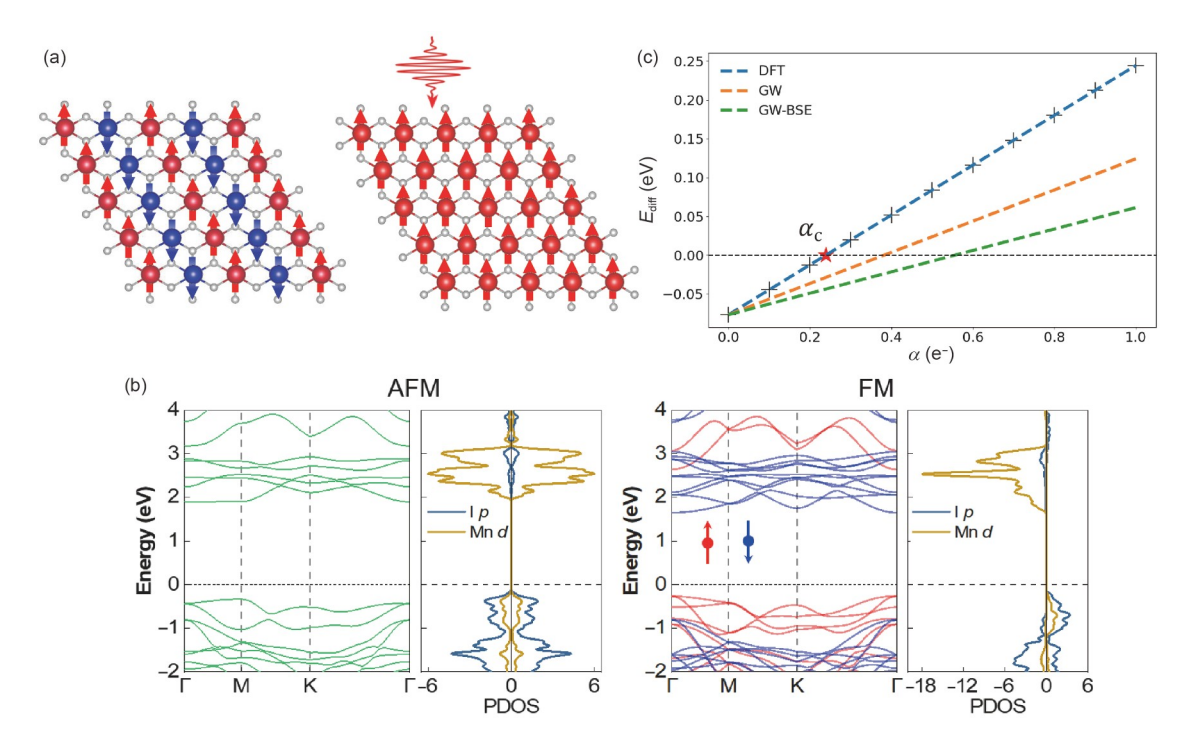


Figure 2 (Color online) (a) Crystal structure of (left) AFM and (right) FM configurations of monolayer MnI_2 from the top view. Red balls and arrows represent spin up Mn atoms, while blue balls and arrows represent spin down Mn atoms. (b) DFT-calculated band structure and density of states of monolayer MnI_2 under (left) AFM and (right) FM configurations. (c) Dependencies of the MnI_2 energy difference between the AFM state and the FM state of DFT, GW, and GW-BSE as a function of the excited electron concentration. The cross-marked points are cDFT calculation results, and the dotted line is derived from the bandgap of DFT and the model mentioned above. The star point represents the number of photoexcited electrons with E'_{diff} =0, which are based on MnI_2 4×4 supercell.

which proves that our theory is universal.

It is well-known that the exciton effect in 2D vdW materials is strong due to the reduced screen effect of electronhole interaction. Therefore, it is important to further verify whether our above conclusion is still valid under the consideration of the exciton effect. Accordingly, we perform a series of first-principles GW and Bethe-Salpeter equation (BSE) [31-33] calculations for MnI₂ monolayer. The calculated bandgaps of AFM (FM) configuration under DFT, GW, GW-BSE methods are 2.23 (1.91) eV, 4.28 (4.08) eV, and 3.17 (3.06) eV, respectively. Note that the value of 3.06 eV is estimated through the scaling law between bandgap and exciton binding energy in 2D semiconductors [34], since the CBM and VBM in the FM configuration belong to different spin channels and our calculations cannot include the electron-hole entanglement between different spins. We emphasize that the calculated results of AFM configuration comply with this law very well. As shown in Figure 2(c), we plot the energy difference between the AFM state and FM state E'_{diff} as a function of the number (α) of the photoexcited electrons. We can see that the FM state will become more stable if enough photocarrier is present even when the exciton effect is included. The linear slope of DFT, GW, GW-BSE curves decreases, which indicates that the electron-hole correlation effect slightly increases the α_c required for MPT.

2.3 Light-induced MPT in other vdW antiferromagnets

In addition to monolayer MnI₂, we will demonstrate that the idea to realize AFM-FM transition using light is general. To further illustrate this, we perform calculations for different 2D antiferromagnets, whose $\frac{E_{\text{diff}}}{G_{\text{diff}}}$ is plotted as a function of α_c in Figure 3 (see details in Supporting Information). Remarkably, we obtain a relational line with slope 1 and intercept 0. These systems vary widely in element types, atomic bond lengths and crystal structures, indicating the generality of our proposed theory. Among these materials, monolayer MnPX₃ (X=Se, S, Te) exhibits Néel antiferromagnetism [35] and valley-dependent optical properties [36]. MnPTe₃ was reported to undergo MPT by varying the electric field [37], here we predict that light illumination is also a very promising approach.

In addition to the monolayer magnetic materials, multilayered materials with interlayer AFM coupling were also reported to display exotic phenomena. For example, giant nonreciprocal second-harmonic generation has been observed in AFM bilayer CrI₃ [38], and modulation of interlayer antiferromagnetism can lead to drastic changes in excitonic transitions in CrSBr bilayers [39]. Therefore, besides the light-induced intralayer AFM-FM transition, we

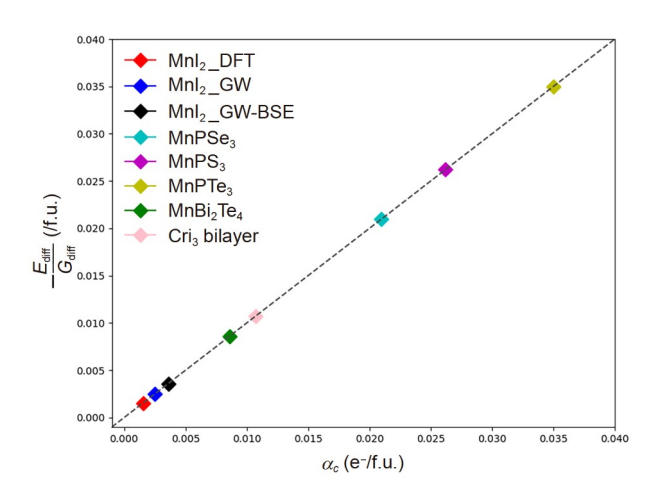


Figure 3 (Color online) Linear relationship between excited electrons number α_c and ratio of ground state energy difference to bandgap difference

 $-\frac{E_{\text{diff}}}{G_{\text{diff}}}$. Calculations cover monolayer vdW materials MnI₂, MnPX₃ (X=Se,

S, Te), and multilayer materials MnBi₂Te₄ and CrI₃ bilayer of HT phase (see Supporting Information for more calculation details).

also perform calculations for several AFM multilayers, including the CrI₃ bilayer and MnBi₂Te₄. We find that light illumination can also change their interlayer AFM coupling to FM coupling. Among them, CrI₃ presents to be an intriguing case. Although bulk CrI₃ is FM, the interlayer coupling becomes AFM when the system is thinned down to a few atomic layers [40], and its interlayer exchange can be tuned by stacking [41-43]. Here, we only consider the high-temperature phase with the AFM interlayer coupling. Our calculations show only a photoelectron concentration of $\alpha_c = 1.073 \times 10^{-2} \text{ e}^{-1}/\text{f.u.}$ (equivalent to $n_e = 2.523 \times 10^{12} \text{ e}^{-1}/\text{cm}^{-1}$) is required for the MPT in bilayer CrI₃. As CrI₃ bilayer can realize the appearance and disappearance of net magnetization through the modulation of light, it is a promising candidate material for next generation photodetectors. Besides, MnBi₂Te₄ was reported to be topological axion state and antiferromagnetism in an even number of layers of films while the quantum anomalous Hall effect and ferromagnetism in the odd number of layers of films [44-49]. We also find that the MPT of MnBi₂Te₄ can be achieved under illumination (Figure 3), similar to the CrI₃ bilayer case.

3 Discussion and conclusions

We note that light can induce MPT in materials as long as the bandgap of the material with ground-state magnetic configuration is larger than that of a higher energy magnetic state. This mechanism is independent of the dimension of materials. For example, 3D CuFeO₂ is reported to be a geometrically frustrated triangular lattice antiferromagnet [50]. In the presence of enough photocarrier, it will become FM (see Supporting Information). The light-induced AFM-insulator

to FM-metal phase transition in Pr_{0.6}La_{0.1}Ca_{0.3}MnO₃ thin films [17,51] can be naturally explained within our theory. In addition, the change of magnetism caused by light will indirectly affect other fundamental properties, such as ferroelectricity and topologic phase. The AFM order in MnI₂ breaks the spatial inversion symmetry and induces ferroelectricity, therefore, the change of magnetic phase under light allows for tuning its ferroelectricity. The AFM-FM phase transition of MnBi₂Te₄ system was suggested to induce the transition from the axion insulator to the Chern insulator phase [39], thus light can be an excellent tool to realize this transformation.

To summarize, we present a general theory of MPT in antiferromagnets, which explains the experimentally observed photoinduced phase transition in manganese oxides. Importantly, we derive a simple linear relationship between critical excited photocarrier concentration α_c and the intrinsic material parameters (including energy difference and bandgap difference between AFM and FM states). The light-induced MPT and this linear relationship are confirmed in a series of first-principles calculations for 2D antiferromagnets, regardless of the types and layers of materials. Our study provides a universal guiding basis for future optoelectronic device designs such as photodetectors, and ultrafast memory devices.

This work was supported by the National Natural Science Foundation of China (Grant Nos. 11991061, 11825403, and 12188101) and the Guangdong Major Project of Basic and Applied Basic Research (Future functional materials under extreme conditions-2021B0301030005). We also acknowledge the support from the National Natural Science Foundation of China (NSAF, Grant No. U1930402).

Supporting Information

The supporting information is available online at http://phys.scichina.com and http://link.springer.com. The supporting materials are published as submitted, without typesetting or editing. The responsibility for scientific accuracy and content remains entirely with the authors.

- C. Gong, and X. Zhang, Science 363, eaav4450 (2019).
- 2 K. S. Burch, D. Mandrus, and J. G. Park, Nature 563, 47 (2018).
- 3 K. F. Mak, J. Shan, and D. C. Ralph, Nat. Rev. Phys. 1, 646 (2019).
- 4 R. Xu, and X. Zou, J. Phys. Chem. Lett. 11, 3152 (2020).
- H. Nojiri, Y. Tokunaga, and M. Motokawa, J. Phys. Colloques 49, C8-1459 (1988).
- 6 S. J. Callori, S. Hu, J. Bertinshaw, Z. J. Yue, S. Danilkin, X. L. Wang, V. Nagarajan, F. Klose, J. Seidel, and C. Ulrich, Phys. Rev. B 91, 140405 (2015), arXiv: 1502.05192.
- 7 Y. Wang, S. S. Wang, Y. Lu, J. Jiang, and S. A. Yang, Nano Lett. 16, 4576 (2016), arXiv: 1608.05164.
- 8 M. Lejman, G. Vaudel, I. C. Infante, I. Chaban, T. Pezeril, M. Edely, G. F. Nataf, M. Guennou, J. Kreisel, V. E. Gusev, B. Dkhil, and P. Ruello, Nat. Commun. 7, 12345 (2016).
- 9 M. Budden, T. Gebert, M. Buzzi, G. Jotzu, E. Wang, T. Matsuyama, G. Meier, Y. Laplace, D. Pontiroli, M. Riccò, F. Schlawin, D. Jaksch, and A. Cavalleri, Nat. Phys. 17, 611 (2021), arXiv: 2002.12835.
- 10 A. Cavalleri, C. Tóth, C. W. Siders, J. A. Squier, F. Ráksi, P. Forget, and J. C. Kieffer, Phys. Rev. Lett. 87, 237401 (2001).

- 11 Y. W. Windsor, D. Zahn, R. Kamrla, J. Feldl, H. Seiler, C. T. Chiang, M. Ramsteiner, W. Widdra, R. Ernstorfer, and L. Rettig, Phys. Rev. Lett. 126, 147202 (2021), arXiv: 2011.07289.
- 12 X. Wang, C. Xiao, H. Park, J. Zhu, C. Wang, T. Taniguchi, K. Watanabe, J. Yan, D. Xiao, D. R. Gamelin, W. Yao, and X. Xu, Nature 604, 468 (2022), arXiv: 2203.07161.
- P. Zhang, T. F. Chung, Q. Li, S. Wang, Q. Wang, W. L. B. Huey, S. Yang, J. E. Goldberger, J. Yao, and X. Zhang, Nat. Mater. 21, 1373 (2022).
- 14 F. Siegrist, J. A. Gessner, M. Ossiander, C. Denker, Y. P. Chang, M. C. Schröder, A. Guggenmos, Y. Cui, J. Walowski, U. Martens, J. K. Dewhurst, U. Kleineberg, M. Münzenberg, S. Sharma, and M. Schultze, Nature 571, 240 (2019).
- 15 P. Scheid, S. Sharma, G. Malinowski, S. Mangin, and S. Lebègue, Nano Lett. 21, 1943 (2021).
- O. Sato, T. Iyoda, A. Fujishima, and K. Hashimoto, Science 272, 704 (1996)
- 17 M. Baran, S. L. Gnatchenko, O. Y. Gorbenko, A. R. Kaul, R. Szymczak, and H. Szymczak, Phys. Rev. B 60, 9244 (1999).
- C. Paillard, S. Prosandeev, and L. Bellaiche, Phys. Rev. B 96, 045205 (2017)
- E. A. A. Pogna, M. Marsili, D. De Fazio, S. Dal Conte, C. Manzoni,
 D. Sangalli, D. Yoon, A. Lombardo, A. C. Ferrari, A. Marini, G.
 Cerullo, and D. Prezzi, ACS Nano 10, 1182 (2016).
- G. Kresse, and J. Furthmüller, Phys. Rev. B 54, 11169 (1996).
- J. P. Perdew, K. Burke, and M. Ernzerhof, Phys. Rev. Lett. 77, 3865 (1996).
- S. L. Dudarev, G. A. Botton, S. Y. Savrasov, C. J. Humphreys, and A. P. Sutton, Phys. Rev. B 57, 1505 (1998).
- 23 C. M. Goringe, D. R. Bowler, and E. Hernández, Rep. Prog. Phys. 60, 1447 (1997).
- 24 Y. S. Hou, H. J. Xiang, and X. G. Gong, Phys. Rev. B 89, 064415 (2014), arXiv: 1310.3590.
- 25 E. Dagotto, T. Hotta, and A. Moreo, Phys. Rep. 344, 1 (2001).
- C. Thomsen, H. T. Grahn, H. J. Maris, and J. Tauc, Phys. Rev. B 34, 4129 (1986).
- T. Sato, H. Kadowaki, and K. Iio, Phys. B: Cond. Matter 213-214, 224 (1995).
- 28 T. Kurumaji, S. Seki, S. Ishiwata, H. Murakawa, Y. Tokunaga, Y. Kaneko, and Y. Tokura, Phys. Rev. Lett. 106, 167206 (2011), arXiv: 1103.5294.
- T. B. Prayitno, and F. Ishii, J. Phys. Soc. Jpn. 88, 104705 (2019), arXiv: 1910.14278.
- 30 H. J. Xiang, E. J. Kan, Y. Zhang, M. H. Whangbo, and X. G. Gong,

- Phys. Rev. Lett. 107, 157202 (2011), arXiv: 1109.1328.
- 31 S. Albrecht, L. Reining, R. del Sole, and G. Onida, Phys. Rev. Lett. 80, 4510 (1998), arXiv: cond-mat/9803194.
- 32 T. Sander, E. Maggio, and G. Kresse, Phys. Rev. B 92, 045209 (2015).
- 33 M. Rohlfing, and S. G. Louie, Phys. Rev. Lett. 81, 2312 (1998).
- 34 Z. Jiang, Z. Liu, Y. Li, and W. Duan, Phys. Rev. Lett. 118, 266401 (2017).
- 35 X. Li, X. Wu, and J. Yang, J. Am. Chem. Soc. 136, 11065 (2014).
- 36 X. Li, T. Cao, Q. Niu, J. Shi, and J. Feng, Proc. Natl. Acad. Sci. USA 110, 3738 (2013), arXiv: 1210.4623.
- 37 B. L. Chittari, Y. Park, D. Lee, M. Han, A. H. MacDonald, E. Hwang, and J. Jung, Phys. Rev. B 94, 184428 (2016), arXiv: 1604.06445.
- 38 Z. Sun, Y. Yi, T. Song, G. Clark, B. Huang, Y. Shan, S. Wu, D. Huang, C. Gao, Z. Chen, M. McGuire, T. Cao, D. Xiao, W. T. Liu, W. Yao, X. Xu, and S. Wu, Nature 572, 497 (2019), arXiv: 1904.03577.
- 39 N. P. Wilson, K. Lee, J. Cenker, K. Xie, A. H. Dismukes, E. J. Telford, J. Fonseca, S. Sivakumar, C. Dean, T. Cao, X. Roy, X. Xu, and X. Zhu, Nat. Mater. 20, 1657 (2021), arXiv: 2103.13280.
- 40 B. Huang, G. Clark, E. Navarro-Moratalla, D. R. Klein, R. Cheng, K. L. Seyler, D. Zhong, E. Schmidgall, M. A. McGuire, D. H. Cobden, W. Yao, D. Xiao, P. Jarillo-Herrero, and X. Xu, Nature 546, 270 (2017), arXiv: 1703.05892.
- N. Sivadas, S. Okamoto, X. Xu, C. J. Fennie, and D. Xiao, Nano Lett. 18, 7658 (2018), arXiv: 1808.06559.
- 42 M. Ezawa, Nat. Mater. 18, 1266 (2019).
- 43 P. Jiang, C. Wang, D. Chen, Z. Zhong, Z. Yuan, Z. Y. Lu, and W. Ji, Phys. Rev. B 99, 144401 (2019), arXiv: 1806.09274.
- 44 C. Liu, Y. Wang, H. Li, Y. Wu, Y. Li, J. Li, K. He, Y. Xu, J. Zhang, and Y. Wang, Nat. Mater. 19, 522 (2020), arXiv: 1905.00715.
- 45 F. Wilczek, Phys. Rev. Lett. 58, 1799 (1987).
- 46 X. L. Qi, T. L. Hughes, and S. C. Zhang, Phys. Rev. B 78, 195424 (2008), arXiv: 0802.3537.
- 47 R. S. K. Mong, A. M. Essin, and J. E. Moore, Phys. Rev. B 81, 245209 (2010), arXiv: 1004.1403.
- 48 A. M. Essin, J. E. Moore, and D. Vanderbilt, Phys. Rev. Lett. 102, 146805 (2009), arXiv: 0810.2992.
- 49 Y. Deng, Y. Yu, M. Z. Shi, Z. Guo, Z. Xu, J. Wang, X. H. Chen, and Y. Zhang, Science 367, 895 (2020), arXiv: 1904.11468.
- 50 F. Wang, and A. Vishwanath, Phys. Rev. Lett. 100, 077201 (2008), arXiv: 0709.3546.
- 51 P. Aleshkevych, M. Baran, R. Szymczak, H. Szymczak, V. A. Bedarev, V. I. Gapon, S. L. Gnatchenko, O. Y. Gorbenko, and A. R. Kaul', Low Temper. Phys. 30, 948 (2004).